Recovery of Burner Acoustic Source Structure from Far-Field Sound Spectra

J. R. Mahan* and J. D. Jones†
Virginia Polytechnic Institute and State University, Blacksburg, Virginia

A method is presented that permits the thermal-acoustic efficiency spectrum in a long turbulent burner to be recovered from the corresponding far-field sound spectrum. An acoustic source/propagation model is used based on the perturbation solution of the equations describing the unsteady one-dimensional flow of an inviscid ideal gas with a distributed heat source. The technique is applied to a long cylindrical hydrogen-flame burner operating over power levels of 4.5-22.3 kW. The results show that the thermal-acoustic efficiency at a given frequency, defined as the fraction of the total burner power converted to acoustic energy at that frequency, is rather insensitive to burner power, having a maximum value on the order of 10^{-4} at 150 Hz and rolling off steeply with increasing frequency. Evidence is presented that acoustic agitation of the flame at low frequencies enhances the mixing of the unburned fuel and air with the hot products of combustion. The paper establishes the potential of the technique as a useful tool for characterizing the acoustic source structure in any burner, such as a gas turbine combustor, for which a reasonable acoustic propagation model can be postulated.

Nomenclature

$A(\omega)$ = transfer function defined by Eq. (14)
c = speed of sound, $\sqrt{\gamma RT}$, m/s
c_p = specific heat at constant pressure, J/K
i = imaginary operator, $\sqrt{-1}$
L = length of heat release zone, m
P = complex ratio of local acoustic pressure magnitude to local steady flow pressure at a given frequency
P_0 = value of P measured in the far field
p = local pressure, kPa
$\bar{p}$ = steady flow component of local pressure, kPa
$\tilde{p}$ = reduced acoustic component of local pressure
Q = complex ratio of local unsteady heat release magnitude to local steady flow heat release at a given frequency, also referred to as the thermal-acoustic efficiency
Q_0 = constant value of Q used in calculating the primitive sound spectra, $\sqrt{2}\times 10^{-5}$
q = local steady heat release, W/m^3
$\bar{q}$ = steady flow component of local heat release, W/m^3
$\tilde{q}$ = reduced unsteady component of local heat release
q_0 = maximum value of local steady heat release, W/m^3
R = gas constant for air, J/K
T = temperature, K; complex ratio of local acoustic temperature magnitude to local steady flow temperature at a given frequency
$\bar{T}$ = steady flow component of local temperature, K
$\tilde{T}$ = reduced acoustic component of local temperature
t = time, s
V = complex ratio of local acoustic velocity magnitude to local steady flow velocity at a given frequency
v = local velocity, m/s
$\bar{v}$ = steady flow component of local velocity, m/s
$\tilde{v}$ = reduced acoustic component of local velocity
x = local position in the burner, m
Z = reduced acoustic impedance defined by Eqs. (12)
z = specific acoustic impedance
α_{ij} = element of the transfer matrix defined by Eqs. (1)
γ = specific heat ratio, c_p/c_v
λ = wavelength of a pressure disturbance, m
ρ = local mass density, kg/m^3
ω = angular frequency, rad/s

Subscripts and Superscripts

I,II = inlet and outlet of the burner, respectively
t,x = partial differentiation with respect to time and axial position, respectively
$( )'$ = differentiation with respect to axial position

Presented as Paper 83-0763 at the AIAA Eighth Aeroacoustics Conference, Atlanta, Ga., April 11-13, 1983; received May 15, 1983; revision received Aug. 15, 1983.

*Associate Professor of Mechanical Engineering (presently Professor of Mechanical and Aerospace Engineering, West Virginia University, Morgantown, W. Va.).
†Instructor of Mechanical Engineering.

Introduction

An important noise source in gas turbine engines is the so-called core noise, most of which is thought to be associated with the combustor. In view of reducing this contribution to the global sound field of a given jet engine, it would be useful to know the spatial and spectral distributions of the predominant sources in the combustion chamber and their relation to the design and operating parameters of the combustor. The technique described in this paper makes such knowledge possible through the use of an acoustic source and propagation model whose coefficients are determined from far-field sound measurements.

The direct measurement of acoustic sources in a burner is complicated by our present lack of understanding of what constitutes a source. For example, we know that local fluctuations of density must produce acoustic waves which propagate through the turbine and tail pipe and into the far field, but which physical processes give rise to these fluctuations in density? The contemporary literature is rich with articles that address this question; see, for example, Refs. 1-5. Unfortunately, the theories given in these articles generally lack sufficient detail to be useful in specifying the relation between the parameters that characterize the construction and operation of a practical burner and the noise that it produces. Indeed, the main value of these studies is that they provide insight into the physical processes producing combustion noise.

Several recent contributions[6-10] approach this question from the other side; that is, the far-field sound level is described directly in terms of the design and operating parameters of the burner or engine through an empirical correlation. The shortcoming of this approach is that such correlations are almost always too specialized, being based on a necessarily limited number of burners (or engines) and operating conditions, to be of broad general significance.

Although very useful for suggesting design changes that might rend a given burner or engine less noisy, this approach provides very little new fundamental knowledge about combustion noise production applicable to a wider range of devices.

The two approaches described in Refs. 1-10 represent opposite extremes that, while addressing real needs in the area of combustion aeroacoustics, do not provide the general engineering tool needed to design "quiet" combustors. The real need is for a model that permits the characterization of the source structure in an arbitrary combustor on the basis of an analysis which includes the design details of the burner. For such a model to be of practical use, at least some experimental results would still be needed to establish the values of certain coefficients to avoid, for example, detailed turbulence calculations. The present contribution represents a first attempt to establish such a model for the source structure in a long turbulent burner on the basis of measured far-field sound spectra.

The general approach in the rather preliminary version of the technique reported here is to assume that all the important acoustic sources in the burner can be represented as a local unsteady heat release whose spatial and spectral distributions depend on the details of construction and operation of the burner. That is, only direct combustion noise is considered.

The general form of the spatial distribution of the sources can be specified from first principles and the appropriate scale factors can be deduced by systematically changing the values of the coefficients of the model until good agreement is obtained between the measured and predicted far-field sound spectra. As a demonstration of the possibilities offered by this method, we have used it to deduce the acoustic source spectrum in a long turbulent burner carefully designed to conform to the assumptions of the acoustic source/propagation model. The results, obtained for a range of power levels, are subject to the reasonable assumption that the local unsteady heat release is proportional to the local steady heat release. Then the variation with frequency of the constant of proportionality is the thermal-acoustic efficiency spectrum.

Definition of the Model

The acoustic source and propagation model is based on a first-order perturbation analysis of the unsteady one-dimensional flow of an inviscid ideal gas with a source term in the corresponding energy equation. When positive the source term represents local combustion heat release and when negative it represents heat loss to the walls. Because the equations describing the acoustic flow are linear, the dependent variables can be related at any frequency of interest by a system of linear algebraic equations,

$$\begin{bmatrix} P_{II} \\ V_{II} \\ T_{II} \end{bmatrix} = \begin{bmatrix} \alpha_{11} & \alpha_{12} & \alpha_{13} & \alpha_{14} \\ \alpha_{21} & \alpha_{22} & \alpha_{23} & \alpha_{24} \\ \alpha_{31} & \alpha_{32} & \alpha_{33} & \alpha_{34} \end{bmatrix} \begin{bmatrix} P_I \\ V_I \\ T_I \\ Q \end{bmatrix} \tag{1}$$

where the indices I and II refer to any two sections of the combustor where the complex values of pressure P, velocity V, and temperature T are defined.‡

The quantity Q in Eqs. (1) is a complex number whose value depends on frequency and that represents the ratio of the unsteady heat release to the steady heat release at that frequency. Thus, it is a thermal-acoustic efficiency whose distribution with frequency we refer to as the acoustic source spectrum. In representing the source term by a single complex number at a given frequency, we are assuming that the local acoustic sources are proportional to the local steady heat release at each frequency. This hypothesis is based on the following reasonable assumptions:

1) Only the local fluctuations of heat release are important in producing the local fluctuations of density that give rise to acoustic waves propagating into the far field as sound (i.e., only direct combustion noise is important).

2) The only significant fluctuations of heat release are those due to the local turbulent mixing of the unburned fuel and air with the hot products of combustion.

3) The local turbulence level (integrated over the burner cross section) is relatively uniform in the combustion zone.

Convincing arguments in favor of the first two assumptions for the type of burner studied here are presented by Legendre in Ref. 5. The third assumption is somewhat more questionable; however, this does not impose a serious limitation on the results obtained if a realistic form is assumed for the axial distribution of steady combustion heat release. For example, in the present study we assume a distribution of the form

$$\bar{q}(x) = q_0 [1 - \cos(2\pi x/L)]/2 \tag{2}$$

where q_0 is the maximum value of the local steady heat release and L the length of the combustion zone. This distribution is similar to that actually found in the experimental burner of the present study. Moreover, Mahan and Kasper[13] have established that the acoustic response of a long burner is not very sensitive to the axial heat release distribution for a given total heat release and flame length. Most of the heat release associated with the distribution represented by Eq. (2) occurs in the vicinity of the peak. Thus, from a practical standpoint, for the third hypothesis to be valid it is sufficient that the turbulence level be fairly uniform in a more limited region of the combustion zone surrounding this peak.

The elements α_{ij} of the transfer matrix of Eqs. (1) are determined by solving the equations that describe the unsteady one-dimensional flow of an inviscid ideal gas with a distributed heat source:

Continuity equation,

$$\rho_t + \rho v_x + v\rho_x = 0 \tag{3}$$

Equation of motion,

$$\rho v_t + \rho v v_x + p_x = 0 \tag{4}$$

Energy equation,

$$\rho c_p T_t + \rho v c_p T_x = p_t + v p_x + q \tag{5}$$

Thermodynamic equation of state,

$$p = \rho R T \tag{6}$$

Calorimetric equation of state,

$$c_p = c_p(T) \tag{7}$$

If one makes the usual assumptions that the solutions p, v, T, and ρ consist of a steady component, which is a function of axial position only, and a very much smaller fluctuating component, which is a function of both axial position and time, and that the steady solution itself also satisfies Eqs. (3-7), there result

$$\bar{v}'/\bar{v} + \bar{p}'/\bar{p} - \bar{T}'/\bar{T} = 0$$

$$\bar{p}\bar{v}\bar{v}' + R\bar{T}\bar{p}' = 0$$

$$\bar{p}\bar{v}c_p\bar{T}' = R\bar{T}\bar{v}\bar{p}' + R\bar{T}\bar{q} \tag{8}$$

and

‡This "transfer matrix" approach was suggested by Krejsa[11] on the basis of a similar analysis by Miles and Raftopoulos.[12]

$$(\tilde{p}-\tilde{T})_t+\bar{v}(\tilde{p}+\tilde{v}-\tilde{T})_x=0$$

$$\tilde{v}_t+(2\tilde{v}-\tilde{T})\bar{v}'+\bar{v}\tilde{v}_x+(R\bar{T}/\bar{v})\tilde{p}_x=0$$

$$\tilde{T}_t+\bar{v}\tilde{T}_x=\left(\frac{\gamma-1}{\gamma}\right)[\tilde{p}_t+\bar{v}\tilde{p}_x-(\tilde{p}+\tilde{v}-\tilde{q})\bar{q}/\bar{p}] \tag{9}$$

In Eqs. (8) and (9) the quantities with overbars ($\bar{}$) are the steady flow variables and the quantities with tildes ($\tilde{}$) the acoustic variables nondimensionalized by the corresponding steady flow variables. The subscripts t and x indicate partial differentiation with respect to those variables and the prime ($'$) associated with the steady flow variables indicates differentiation with respect to the axial position.

Equations (8) can be integrated directly for a specified axial distribution of steady heat release $\bar{q}(x)$ beginning at any section, the burner inlet for example, where initial values of the pressure, temperature, and velocity are known. Once these equations have been solved the variable coefficients in the acoustic equations are known. In order to solve the acoustic Eqs. (9), periodic solutions are assumed of the form

$$\tilde{p}=Pe^{i\omega t}, \qquad \tilde{v}=Ve^{i\omega t}, \qquad \tilde{T}=Te^{i\omega t}$$

with

$$\tilde{q}=Qe^{i\omega t} \tag{10}$$

where the complex variables P, V, T, and Q are functions of axial position only. When these assumed forms are introduced into Eqs. (9), there result the ordinary differential equations

$$i\omega(P-V)+\bar{v}(P'+V'-T')=0$$

$$i\omega V+(2V-T)\bar{v}'+\bar{v}V'+R\bar{T}P'/\bar{v}=0 \tag{11}$$

and

$$i\omega T+\bar{v}T'=\left(\frac{\gamma-1}{\gamma}\right)[i\omega P+\bar{v}P'-(P+V-Q)\bar{q}/\bar{p}]$$

which can be integrated numerically from any section where the initial values are known.

Unfortunately, a straightforward integration of the acoustic Eqs. (11) is not possible. Unlike the case of the steady flow equations (8) for which $\bar{q}$ is specified and the values of $\bar{p}$, $\bar{v}$, and $\bar{T}$ are known at the burner inlet, there is no section where the complex values of P, V, and T are known. It is, of course, the variation with frequency of the thermal-acoustic efficiency Q that is sought in this study. It is for this reason that we have adopted the transfer matrix approach represented by Eqs. (1). We can find the elements α_{ij} of the matrix by integrating Eqs. (11) four times, each time using a different but linearly independent set of arbitrary initial conditions P_I, V_I, and T_I and the source function Q. If, for example, for the first integration the initial values at the inlet of the burner are assumed to be $P_I=1$ and $V_I=T_I=0$, and the source function is assumed to be $Q=0$, the first column of coefficients can be expressed in terms of the solution obtained by integrating along the burner to the open end of the exhaust pipe, i.e., $\alpha_{1I}=P_{II}$, $\alpha_{2I}=V_{II}$, and $\alpha_{3I}=T_{II}$.

Once the elements of the transfer matrix have been determined for a given frequency, there remain three algebraic equations in seven unknowns: the values of P, V, and T at each end of the burner and the value of Q. Three additional equations can be written in terms of the measured acoustic impedance at either end of the burner,

$$Z_I=P_I/V_I \quad \text{and} \quad Z_{II}=P_{II}/V_{II} \tag{12}$$

and the isentropic condition at the burner inlet,

$$T_I=\left(\frac{\gamma-1}{\gamma}\right)P_I \tag{13}$$

The final equation needed to have a determinant system is the relation between the pressure fluctuation at the open end of the exhaust pipe and the acoustic pressure measured at the same frequency in the far field,

$$P_{II}(\omega)=A(\omega)P_0(\omega) \tag{14}$$

where $A(\omega)$ is the appropriate transfer function. In principle, we can now compute Q using Eqs. (1) and (12-14) for any frequency ω for which we have measured P_0.

Implementation

The experimental apparatus is shown in Fig. 1. The fuel (hydrogen) enters the combustion chamber through a small sonic orifice in the center of a disk around which air is introduced with a swirl component of velocity. The use of a sonic orifice assures that the acoustic-scale pressure fluctuations in the burner cannot modulate the injection of hydrogen, thus avoiding the possibility of combustion "feed" instability. The air, which flows through a silencer before entering the combustion chamber, is metered by a calibrated rotameter. The wake created by the disk and the swirl component of velocity stabilize the flame.

The products of combustion are vented into an anechoic chamber through an exhaust pipe having the same inside diameter, 54.6 mm, as the combustion chamber. The burner, including the exhaust pipe, is 1.53 m long and penetrates 0.78 m into the anechoic chamber. The flanges that couple the fuel and air injection manifold and the exhaust pipe to the combustion chamber are water cooled, as is that portion of the exhaust pipe outside the anechoic chamber. The anechoic chamber measures $2.3\times2.6\times4.0$ m and is ventilated by a silenced blower whose capacity limits the power level of the burner to a maximum of around 25 kW. The burner power level is computed from the hydrogen flow rate measured using a calibrated rotameter and assuming complete combustion.

Two 1.27 cm microphones are located in the anechoic chamber at a distance of 1.5 m from the open end of the exhaust pipe, one on the axis of the burner and the other at an angle of 45 deg in the vertical plane above the axis. These microphones are connected to amplifiers through suitable preamplifiers. A fast Fourier transform analyzer interacts with a graphics terminal to produce autospectra from the sound pressure signals measured by the microphones. The system is calibrated using a pistonphone.

Measurement of the Acoustic Impedance

The classical impedance tube method was used to measure the acoustic impedance at each end of the burner. The

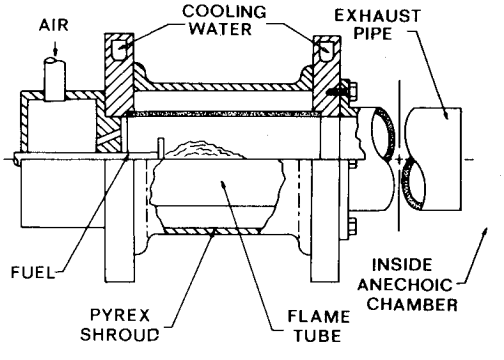

Fig. 1 Cutaway view of the experimental burner.

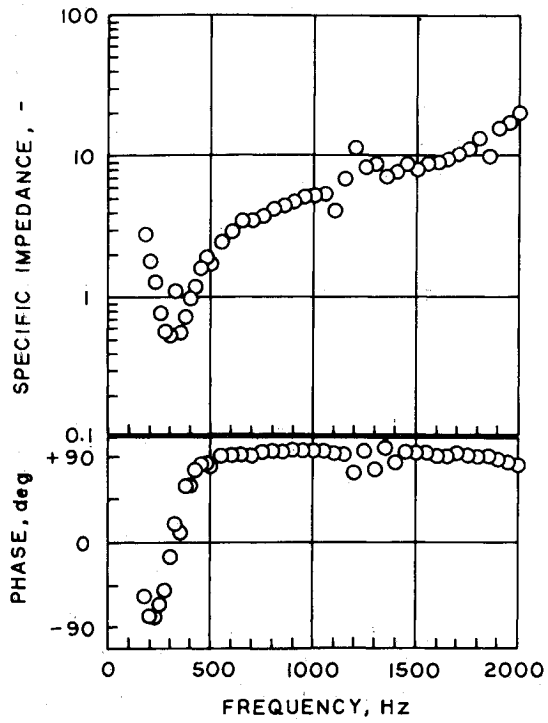

Fig. 2 Specific impedance measured at the closed end of the burner.

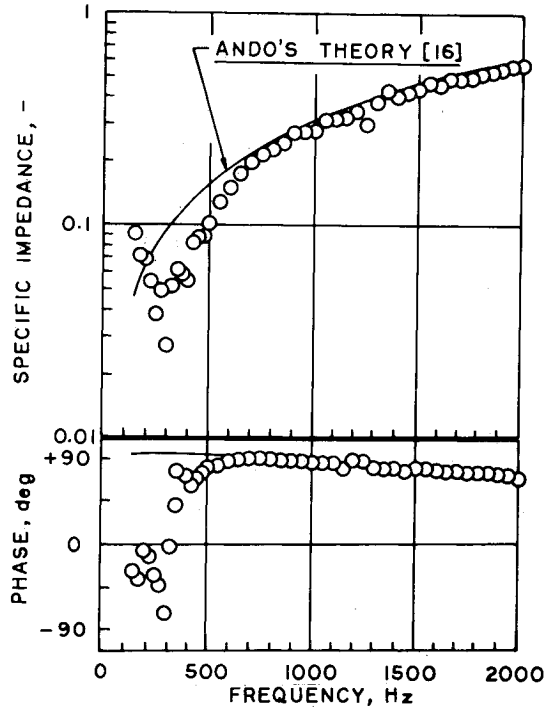

Fig. 3 Specific impedance measured at the open end of the burner (the solid line is Ando's[16] theory).

measurements were made in the cold burner without flow and the results extended to the cases with combustion using the relation

$$Z=\rho c z\bar{v}/\bar{p} \tag{15}$$

where ρc is the characteristic impedance corresponding to the local conditions with combustion and z the specific impedance measured without combustion. There is no need in this study to correct the impedance for flow effects because the Mach number is always less than 0.02 in the burner.

There can be little doubt of the validity of Eq. (15) at the burner inlet because the conditions there never differ greatly from those without combustion. However, the conditions at the outlet of the exhaust pipe vary significantly with the power level. Indeed, the rather steep axial temperature gradient existing at the end of the burner must cast doubt on the validity of using this method to determine the impedance there. Is it possible that these gradients alter the degree to which a circular pipe radiates acoustic energy? Two recent studies[14,15] of this question seem to indicate that this is not the case, although more research is needed to confirm this conclusion.

The impedances measured at the two ends of the burner are shown in Figs. 2 and 3. The theoretical impedance of Ando[16] also appears in Fig. 3, which shows the magnitude and phase of the specific impedance at the open end of the exhaust pipe. The agreement between experiment and theory is very good above 600 Hz. The divergence that begins below 600 Hz is probably due to the departure of the chamber from anechoic conditions at low frequencies.

Determination of the Source Spectra

A block diagram of the procedure for calculating the thermal-acoustic efficiency spectrum is shown in Fig. 4.

The procedure for solving Eqs. (1) with Eqs. (12-14) is as follows. First, the steady flow equations are integrated starting at the burner inlet, where the pressure, velocity, and temperature are known, subject to a specified axial heat-transfer distribution. In principle this distribution is determined from the known combustion heat release distributed according to Eq. (2), the measured heat loss to the flanges and the cooled portion of the exhaust pipe, and the value of the heat loss to the uncooled portion of the exhaust pipe necessary to obtain the measured gas temperature at the open end. In practice, however, a better agreement can be obtained between the frequencies at which peaks occur in the calculated and measured pressure spectra by slightly adjusting the assumed heat loss to the uncooled portion of the exhaust pipe.

Next, an arbitrary value for the thermal-acoustic efficiency Q is assumed whose magnitude is constant at Q_0. The six equations in six unknowns that remain after the value of Q_0 has been specified are then solved for each frequency of interest. For these calculations, the flame is divided axially into 20 source elements. This step was deemed necessary because of the finite length of the flame. It is probable that a single source element would be adequate for a sufficiently short flame. Then in order to have incoherent sources, 20 spectra are calculated corresponding to a source at each of the source locations along the length of the flame. These 20 spectra are then added together and multiplied by $A(\omega)$ to form the primitive far-field spectrum. The use of incoherent sources is consistent with the idea that the sources are due to turbulence.

After having thus obtained a primitive pressure autospectrum whose peaks align with those of the measured pressure autospectrum, the corresponding source spectrum can be calculated from

$$Q(\omega)=P_0(\omega)Q_0/P(\omega) \tag{16}$$

where $P_0(\omega)$ is the measured sound spectrum and $P(\omega)$ the calculated primitive far-field sound spectrum corresponding to Q_0. Equation (16) is based on the fact that Eqs. (1) are linear. In the results presented in this paper a value of unity has been assumed for the transfer function $A(\omega)$ in Eq. (14). This seems justified in view of the relative proximity of the field microphone to the open end of the pipe and the limited frequency range.

Results

The experimental sound pressure autospectra for burner power levels of 4.5, 10.0, and 22.3 kW are shown in Fig. 5. These spectra were obtained from the on-axis microphone,

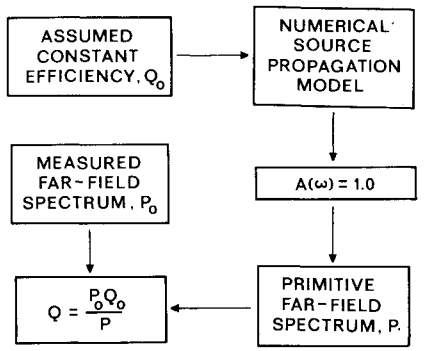

Fig. 4 Block diagram for calculating the thermal-acoustic efficiency spectrum.

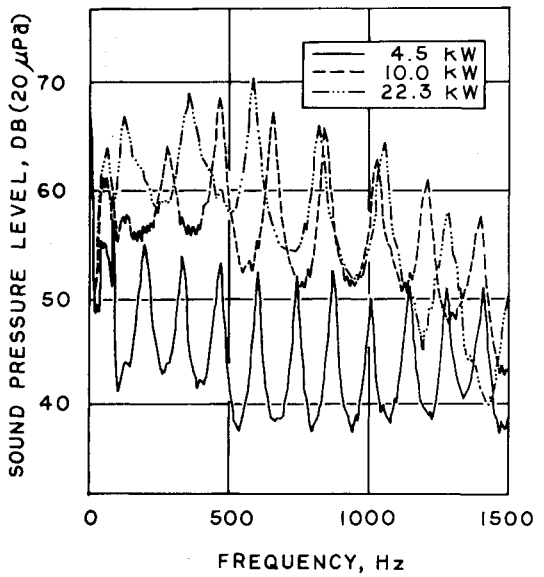

Fig. 5 Measured far-field sound spectra.

but the spectra from the microphone at an angle of 45 deg from the axis are nearly identical. There is a significant difference in sound levels between the 4.5 and 10.0 kW cases, while the difference between the 10.0 and 22.3 kW cases is relatively minor. The general trend in each of the three spectra is for the pressure level to roll off with the frequency with a slope that increases with the burner power level. Of course, the peaks in the spectra correspond to the resonant ("organ pipe") frequencies of the burner.

The corresponding primitive spectra, calculated using a value of 1.41×10^{-5} for the magnitude of Q_0, are shown in Fig. 6. These calculations are limited to 150 Hz at low frequencies because the terminating impedances at the ends of the burner could not be measured with confidence below this frequency.

There are four obvious differences between the measured spectra of Fig. 5 and the calculated spectra of Fig. 6:

1) The measured spectra generally decrease with frequency, while the calculated spectra generally increase.

2) The measured spectra have simple peaks, while the calculated spectra have double peaks above a certain frequency.

3) The calculated spectra have larger peak-to-valley differences (and sharper peaks) than the measured spectra.

4) The general depression in the spectra around 700-900 Hz (depending on the burner power level) is much more pronounced in the calculated spectra than in the measured spectra.

The first difference is a direct consequence of the difference between the actual source spectra in the burner and the

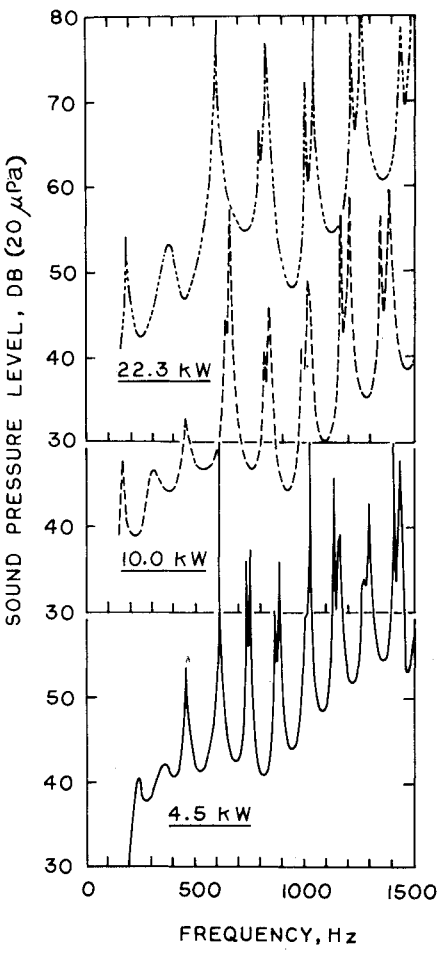

Fig. 6 Primitive far-field sound spectra.

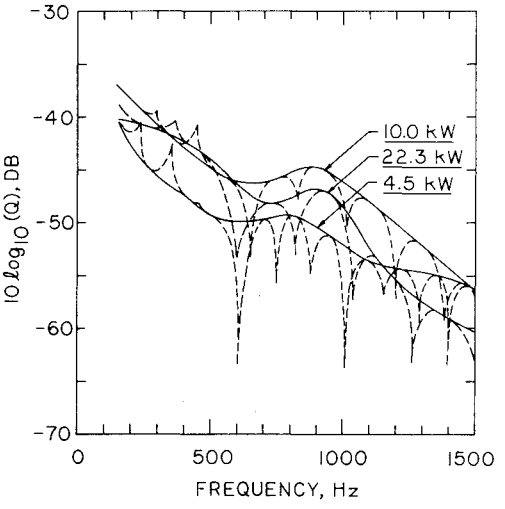

Fig. 7 The source spectra.

assumed constant source spectrum Q_0, whereas the other three differences are artifacts of the acoustic model.

The double peaks in the calculated spectrum occur because there are two acoustic lengths in the model that produce resonances in the frequency range of the calculations. These are the distance between the two ends of the burner and the distance between the open end of the burner and the steep temperature gradient associated with the combustion heat release. The sharp variation of the characteristic impedance ρc associated with this temperature gradient produces a significant reflection of acoustic energy at sufficiently short

wavelengths. The fact that no obvious secondary peaks appear in the measured spectra indicates that the one-dimensionality assumed by the acoustic model is not strictly valid in the flame zone. Indeed, the flame does not fill the flame tube in the actual burner, thus leaving an annular region surrounding the flame through which acoustic waves can propagate without being directly influenced by the steep axial temperature gradient in the flame.

One reason the calculated spectra have larger peak-to-valley differences (and sharper peaks) than the measured spectra is that the latter are averaged, finite analysis interval spectra, whereas the former are based on an infinitesimal analysis interval. Another reason is that the only acoustic loss mechanism in the model is the radiation resistance at either end of the burner. In the actual burner, there are other loss mechanisms associated with viscosity and thermal conductivity that further limit the amplitudes of the resonant peaks. These secondary losses are much less important in determining the values of the spectra at antiresonance, i.e., when the burner is detuned. Thus, the values of the source spectra calculated at antiresonance using Eq. (16) are much more representative than those calculated at or near resonance.

The general depression, or dip, in the spectra especially evident at antiresonance around 700-900 Hz, depending on the burner power level, is a consequence of the Rayleigh criterion,[17] the integral form of which requires that pressure disturbances of wavelength λ be amplified according to the value of

$$\int_0^{\lambda} p(x) \cdot q(x)\,dx$$

where $p(x)$ is the local acoustic pressure variation and $q(x)$ the local unsteady heat transfer. The dot $(\cdot)$ indicates the multiplication of two complex variables; that is, the phase relation between p and q must be considered in evaluating the integral. A pressure disturbance of wavelength λ will be amplified for positive values of the integral and damped for negative values, while remaining unaffected for a value of zero. Then the depression in the sound pressure autospectra especially evident in the calculated spectra is due to the first alignment with increasing frequency of a standing wave pressure node with the peak in the heat release distribution, a situation that minimizes the value of this integral. The fact that this effect is barely noticeable in the measured spectra indicates once again the inadequacy of a one-dimensional model in the flame zone; in reality, only that portion of the acoustic wave in the center of the tube is subject to the amplification required by Rayleigh's criterion.

The source spectra calculated using Eq. (16) and the measured and calculated sound pressure autospectra of Figs. 5 and 6 appear in Fig. 7. The ordinate is in decibels referred to the burner power level; that is, $dB = 10 \log_{10}(Q)$ where Q is the thermal-acoustic efficiency given by Eq. (16). The dashed lines represent the actual source spectra calculated using Eq. (16) but ignoring the secondary peaks in the theoretical spectra, and the solid lines are smooth curves joining the values of the source spectra corresponding to the antiresonances of the sound pressure spectra. Following the above arguments concerning the differences between the measured and calculated sound spectra, the solid curves are more representative of the actual source spectra than the dashed curves. This is especially true at the higher frequencies where secondary loss mechanisms would be increasingly important. The "humps" occurring in all three spectra between 700 and 900 Hz are a result of the departure from one-dimensionality in the flame zone of the real burner, as explained above, and thus are not really significant.

It is not surprising to see that the source spectra roll off rather steeply with frequency; this is consistent with the idea that the most important source mechanism is the turbulent mixing of the unburned fuel and air with the hot products of combustion. The fact that at 1500 Hz the source spectra are down nearly 20 dB from their values at 150 Hz justifies the decision to limit the study to this frequency range. All three source spectra decrease an order of magnitude between 150 and 500 Hz. Thus, the most significant source activity is limited to the same frequency range, 0-500 Hz, where it is typically found in jet and open-flame noise studies.

The three source spectra lie within a 5 dB band and in fact intersect at several frequencies. In general, the low burner power case produces the lowest source spectrum, but the high power case does not produce the highest spectrum. The low burner power spectrum even rises above the high burner power spectrum beyond 1100 Hz. The combined uncertainty of the experimental and theoretical methods employed in this study is such that it is reasonable to conclude that the thermal-acoustic efficiency Q is relatively insensitive to burner power level. This efficiency has a peak value on the order of 10^{-4} at 150 Hz and decreases about two orders of magnitude for a one order of magnitude increase in frequency.

An interesting aspect of these source spectra is that in all three cases there is a critical frequency near 500 Hz, above which the resonant peaks in the corresponding sound pressure spectra produce sharp depressions in the source spectra (dashed lines), but below which the resonant peaks in the sound spectra produce sharp peaks in the source spectra. The sharp depressions have already been explained in terms of the exaggerated resonant peaks in the theoretical sound pressure spectra, but how can the peaks in the source spectra below 500 Hz be explained? A possible explanation is that the mixing process is enhanced at low frequencies by the acoustic agitation of the flame. This is consistent with measurements of flame transfer functions reported in the literature,[18] which show that flames respond somewhat like amplified first-order systems, with a relatively flat response up to a critical frequency beyond which the response rolls off steeply with frequency.

Conclusions

A method has been presented that permits the acoustic source structure in a long turbulent burner to be recovered from far-field sound pressure spectra. The procedure is based on solution of the linearized equations that describe the unsteady one-dimensional flow of an inviscid ideal gas in which acoustic sources are represented by an unsteady component of combustion heat release. The principal conclusions that can be drawn from this experimental study may be stated as follows:

1) The thermal-acoustic efficiency Q is relatively insensitive to the burner power level and has a peak value at low frequencies on the order of 10^{-4}.

2) The thermal-acoustic efficiency decreases monotonically by an order of magnitude over the frequency range of 150-500 Hz.

3) There is evidence that the turbulent mixing of the unburned fuel and air with the hot products of combustion is enhanced near resonance by acoustic agitation below a critical frequency around 500 Hz.

The study also establishes the need for an improved source/propagation model that is two-dimensional in the combustion zone and includes loss mechanisms other than the radiation resistance at the ends of the burner. The most important conclusion, however, is that the general approach is sound and is a potentially very useful tool for characterizing the source spectra in any burner, including a gas turbine combustor, for which a reasonable acoustic propagation model can be postulated.

Acknowledgments

The authors are grateful to the NASA Lewis Research Center for support of this research under Grant NAG3-124,

and especially to Mr. E. A. Krejsa at NASA Lewis for his valuable contributions to this work. A debt of gratitude is also owed to the French Office of Aerospace Research (ONERA), where the first author spent the 1982-83 academic year, for their support of the analysis which appears in this paper. Finally, the authors would like to thank Mr. D. E. Parekh for his assistance in the experimental phase of this research.

References

[1]Strahle, W. C., "On Combustion Generated Noise," *Journal of Fluid Mechanics*, Vol. 49, Sept. 1971, pp. 399-414.

[2]Strahle, W. C., "Some Results in Combustion Generated Noise," *Journal of Sound and Vibration*, Vol. 23, July 1972, pp. 113-125.

[3]Dowling, A. P., "Mean Temperature and Flow Effects on Combustion Noise," AIAA Paper 79-0590, March 1979.

[4]Cumpsty, N. A., "Jet Engine Combustion Noise: Pressure Entropy and Vorticity Perturbations Produced by Unsteady Combustion or Heat Addition," *Journal of Sound and Vibration*, Vol. 66, Oct. 1979, pp. 527-544.

[5]Legendre, R., "Bruit de combustion," *La Recherche Aérospatiale*, Vol. 1980-5, Sept.-Oct. 1980, pp. 360-371.

[6]Shivashankara, B. N. and Crouch, R. W., "Combustion Noise Characteristics of a Can-Type Combustor," AIAA Paper 76-578, July 1976.

[7]Mathews, D. C. and Rekos, M. F., "Prediction and Measurement of Direct Combustion Noise in Turbopropulsion Systems," *Journal of Aircraft*, Vol. 14, Sept. 1977, pp. 850-859.

[8]Strahle, W. C. and Muthukrishnan, M., "Correlation of Combustor Rig Sound Power Data and Theoretical Basis of Results," *AIAA Journal*, Vol. 18, March 1980, pp. 269-274.

[9]Shivashankara, B. N., "Gas Turbine Core Noise Source Isolation by Internal-to-Far-Field Correlations," *Journal of Aircraft*, Vol. 15, Sept. 1978, pp. 597-600.

[10]Strahle, W. C. and Shivashankara, B. N., "Combustion Generated Noise in Gas Turbine Combustors," *Journal of Engineering for Power*, Vol. 98, April 1976, pp. 242-246.

[11]Krejsa, E. A., Personal communication, NASA Lewis Research Center, July 1982.

[12]Miles, J. H. and Raftopoulos, D. D., "Spectral Structure of Pressure Measurements Made in a Combustion Duct," *Journal of the Acoustical Society of America*, Vol. 68, Dec. 1980, pp. 1711-1722.

[13]Mahan, J. R. and Kasper, J. M., "Influence of Heat Release Distribution on the Acoustic Response of Long Burners," ASME Paper 79-DET-31, Sept. 1979.

[14]Fricker, N. and Roberts, C. A., "The Measurement of the Acoustic Radiation Impedance of the Open End of a Thick Walled Tube with Hot Flow," *Acustica*, Vol. 38, Aug. 1977, pp. 124-130.

[15]Cummings, A., "High Temperature Effects on the Radiation Impedance of an Unflanged Duct Exit," *Journal of Sound and Vibration*, Vol. 52, May 1977, pp. 299-304.

[16]Ando, Y., "On the Sound Radiation from Semi-Infinite Circular Pipe of Certain Wall Thickness," *Acustica*, Vol. 22, 1969-70, pp. 219-225.

[17]Lord Rayleigh, *Theory of Sound*, 2nd ed., Vol. 2, Dover Publications, New York, 1945, p. 226.

[18]Riley, J. F., Leonard, R. G., and Goldschmidt, V. W., "A Transfer Function and Experimental Analysis of Feedback Excited Oscillations in Gas Flames," Purdue University, West Layfette, Ind., Rept. 8 HL 74-29, 1974.